Lai, D. and Chen, Q. 2016. "A two-dimensional model for calculating heat transfer in the human body in a transient and non-uniform thermal environment," *Energy and Buildings*, 118: 114-122.

A Two-Dimensional Model for Calculating Heat Transfer in the Human Body in a Transient and Non-Uniform Thermal Environment

Dayi Lai[1], Qingyan Chen[2,1*]

[1]School of Mechanical Engineering, Purdue University, West Lafayette, IN 47907, USA

[2]Tianjin Key Lab of Indoor Air Environmental Quality Control, School of Environmental Science and Engineering, Tianjin University, Tianjin 300072, China

*Corresponding author: Qingyan Chen

Phone: +1-765-496-7562, Email: yanchen@purdue.edu

Abstract

A thermal model for the human body is used to assess the temperature of the body and a person's thermal comfort level. Most models available in the literature were developed for a uniform thermal environment and have limited applications. This study developed a 12-segment model for transient and non-uniform surrounding conditions by considering two-dimensional heat transfer in each segment of a human body. This heat transfer included convection, radiation, and evaporation on bare skin and skin covered with clothing. The model allows non-uniform clothing insulation across different body segments. The heat transfer between two body segments was estimated from blood circulation through counter-current heat exchange. This study evaluated the model's performance for subjects with and without clothing under a wide range of transient and non-uniform thermal environmental conditions. Good agreement was observed between the measured and calculated skin and rectal temperatures, although there were small discrepancies. The two-dimensional model developed in this study is a step forward in predicting thermal comfort under transient and non-uniform environmental conditions.

Keywords: Heat transfer; Transient and non-uniform environment; Human body; Thermal comfort

Highlights:

This study developed a two-dimensional heat transfer model for a 12-segment human body.

The model considered transient and non-uniform convection, radiation, and evaporation around the body.

The model considered the impact of local clothing insulation on heat transfer.

The model was validated for predicting skin and body core temperatures under a wide range of thermal conditions.

1. Introduction

Our daily life is spent in a variety of indoor and outdoor spaces. When we are indoors, we try to control the thermal environment in order to be comfortable. In outdoor spaces, we try to maintain comfort by adjusting our clothing level and metabolic rate. Regardless of the type of space, a designer needs a suitable model to determine whether or not a person in the designed space is comfortable.

Many different thermal comfort models are available, some of which were developed for indoor spaces and the rest for outdoor spaces. Essentially, all of these models are based on the thermal balance between the human body and the surroundings. For example, Fanger's predicted mean vote (PMV) model [1], Gagge's standard effective temperature (SET) model [2], and Hoppe's physiological equivalent temperature (PET) model [3] established the heat balance between a single-segment human body and a uniform surrounding environment. The assumptions of single segmentation and uniform thermal environment are acceptable in most indoor spaces because thermal parameters such as airflow speed and the radiant field around the human body do not change greatly. For other spaces, such as outdoor spaces, these assumptions may not be acceptable and would lead to uncertainties in predicting thermal comfort. For example, Lai et al. [4] found that the PMV model overestimated the thermal sensation by a factor of 1.3 for outdoor spaces. This discrepancy may have been due to an incorrect estimation of the heat transfer between the lumped single segment of the human body and the uniform environment. In the outdoor spaces investigated, the thermal environment was highly non-uniform because of rapid changes in wind speed and direction and in solar radiation. These non-uniformities would have led to different rates of heat exchange in different human body segments. To better estimate the temperature and physiological responses of human bodies, heat transfer should be accurately determined by calculating the transfer in different body segments.

Stolwijk [5] developed the first multi-segment model. He divided a human body into six segments and proposed equations for controlling the thermoregulation processes. Stolwijk's model is a milestone in the development of multi-segment thermal models for the human body [6], but it has limitations. For example, the model developed the thermoregulation equations on the basis of limited data, it used a constant blood temperature, and it assumed constant radiation and convection between the body and the environment.

Numerous researchers have improved Stolwijk's model by addressing these limitations. Huizenga et al. [7] enhanced the blood heat transfer calculation by considering the counter-flow heat exchange in arteries and veins in extremities. They also improved the convection and radiation heat transfer calculations. Fiala [8-11] improved the thermoregulation processes by using experimental data on sweating, shivering, vasoconstriction, and dilation. Although the improvements by these researchers have made the multi-segment model more accurate, there are still many uncertainties, for example, the neglecting of angular heat conduction and the arterial blood temperature drop along the extremities. Such uncertainties may lead to inaccuracy in predicting the temperature of the human body. Furthermore, in the previous models [7-11], no method was provided for determining the level of clothing insulation at local segments. Although the multi-segment models were developed for a non-uniform thermal environment, they were only validated under uniform conditions in previous studies.

The present study aimed to develop a multi-segment model based on Fiala's work with the following improvements:

- conduction in both radial and angular directions,
- arterial blood temperature drop along the extremities, and
- a method for quantifying clothing insulation at local segments.

This study also validated the improved model for a non-uniform thermal environment.

2. Model description

The formulation of a multi-segment model started with the "construction" of a human body. This investigation used the bio-heat transfer equation [12] to describe the heat transfer inside the body. The heat from metabolism was distributed to different body parts by conduction in bone, muscle, fat, and skin and by convection through blood circulation. Finally, the heat was transferred from the skin surface to the surrounding environment by means of convection, radiation, and evaporation. When the body parts were covered by clothing, it provided resistance to heat and mass transfer between the skin and the surroundings. In addition to heat exchange on the skin surfaces, heat and mass transfer between the body and the surroundings occurred through respiration. The bio-heat transfer equation can be discretized to solve for the temperature distribution of the human body.

2.1. Construction of a human body

Our construction of a human body used Fiala's representation of the physiological and physical data for an average person [11]. As shown in Figure 1(a), this study divided the body into 12 segments: the head, face, neck, shoulder, thorax, abdomen, upper arms, lower arms, hands, upper legs, lower legs, and feet. These segments were defined on the basis of the geometric characteristics, physiological composition, and clothing variation of each segment. All the segments were modeled as cylinders, and cylindrical coordinates were used to represent them. The temperature gradient along the radial direction and the asymmetric boundary condition along the angular direction were considered, but the temperature in the longitudinal direction was assumed to be uniform. The heat transfer between body segments was determined only by blood circulation. As shown in Figure 1(b), each segment consisted of four or five concentric layers, which were a combination of the following seven tissue materials: brain, lung, viscera, bone, muscle, fat, and skin. The detailed dimensions of each segment were the same as those used by Fiala et al. [11].

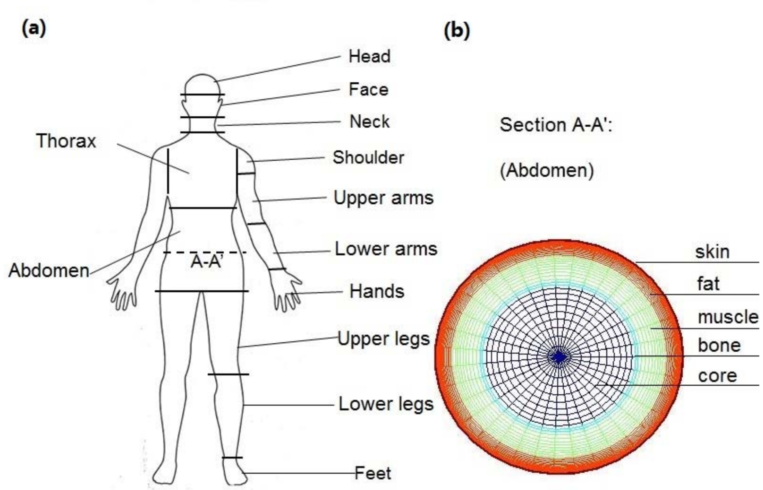

Fig. 1. (a) Division of the human body into segments (left) and (b) layer formulation for the abdomen segment (right).

2.2. Heat transfer within the human body

This study used the bio-heat transfer equation [12] to model the heat transfer within the human body:

$$\rho c \frac{\partial T}{\partial t} = \nabla \cdot (k \nabla T) + q_m + \omega_{bl} \rho_{bl} c_{bl} (T_{bla} - T) \quad (1)$$

where ρ is the tissue density (kg/m^3), c the specific heat of the tissue ($J/kg/K$), T the tissue temperature (K), t the time (s), k the tissue thermal conductivity ($W/m/K$), q_m the metabolic heat generation (W/m^3), ω_{bl} the blood perfusion rate (s^{-1}), ρ_{bl} the density of the blood (kg/m^3), c_{bl} the specific heat of the blood ($J/kg/K$), and T_{bla} the arterial blood temperature (K). The term on the left side of Eq. (1) is the heat storage, which is equal to the summation of the three terms on the right side of the equation: the conduction, heat generation, and blood perfusion, respectively. We applied the same ρ, c, and k values from Fiala et al. [11] to this study. The variable ω_{bl} is at a constant value when the human body is in a thermally neutral state. When the body deviates from thermal neutrality, the value of ω_{bl} changes because of vasoconstriction and dilation [11]. The variables q_m and T_{bla} are unknown in Eq. (1). In order to solve the equation for T, these variables should be determined as follows.

2.3. Metabolism

The metabolic heat generation q_m is equal to the summation of the basal metabolic rate ($q_{m,bas,0}$) and additional heat generation due to work ($q_{m,w}$), shivering ($q_{m,sh}$), and change in the body's thermal state ($\Delta q_{m,bas}$):

$$q_m = q_{m,bas,0} + q_{m,w} + q_{m,sh} + \Delta q_{m,bas} \quad (2)$$

where $q_{m,bas,0}$ is constant according to Fiala et al. [11]. The value of $q_{m,w}$ can be determined from the workload on the human body; a heavier workload would lead to greater heat generation in the muscle layers. The $q_{m,sh}$ in Eq. (2) is the heat generated by shivering in the muscle layers to maintain the body core temperature. Finally, the $\Delta q_{m,bas}$ can be calculated according to the thermal state of the body. The human body produces more heat when its thermal state is higher than neutrality, and vice versa. The detailed formulation of $q_{m,w}$, $q_{m,sh}$, and $\Delta q_{m,bas}$ can be found in Fiala et al. [11].

In the respiratory tract, q_m is reduced by respiration heat loss. This heat loss can be modeled according to Fanger [13] and is distributed to the various body elements of the respiration channel according to Fiala et al. [11]: 45% to the face muscles, 25% to the muscles in the neck, and 30% to the lungs.

2.4. Blood circulation

The arterial temperature, T_{bla} in Eq. (1), can be calculated by the use of a blood circulation model. Blood flows out from the central blood pool through the central artery and returns to the pool through the central vein. In the central segments (head, face, neck, thorax, and abdomen), heat transfer is ineffective. Because of the relatively large blood flow and short vessel length, T_{bla} is equal to the blood pool temperature T_{blp} for these segments [7]. In the extremity segments (shoulders, upper arms, lower arms, hands, upper legs, lower legs, and feet), because of the counter-current heat exchange between artery and vein, T_{bla} decreases along the direction of arterial blood flow. Fig. 2 shows the determination of T_{bla} in the lower extremities. In the upper legs, T_{bla} still equals T_{blp} because the arterial blood has just flowed out of the central segment (abdomen). In the lower legs, T_{bla} is reduced by $\Delta T_{bla,upper\ legs}$ as a result of the counter-current heat exchange in the upper legs. In the feet, T_{bla} is even lower, and the reduction in temperature is due to the counter-current heat exchange in the upper legs and lower legs ($\Delta T_{bla,upper\ legs} + \Delta T_{bla,lower\ legs}$). The arterial temperature in the upper extremity segments is determined in a similar way.

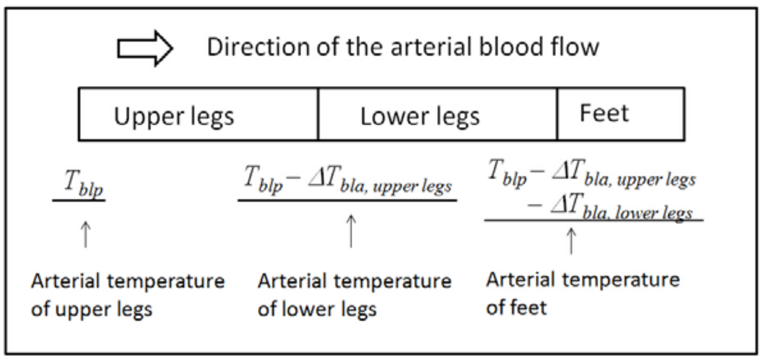

Fig. 2. Determination of arterial temperature in lower extremity segments.

The ΔT_{bla} for a segment is related to the net counter-current heat exchange Q_x (W):

$$Q_x = \rho_{bl} c_{bl} \sum_{layers} (\omega_{bl} V) \cdot \Delta T_{bla} \tag{3}$$

where V is the volume of a layer within the segment (m^3), and $\Sigma(\omega_{bl}V)$ represents the volumetric flow rate of blood (m^3/s). The Q_x can be calculated by the equation proposed by Gordon [14]:

$$Q_x = h_x (T_{bla} - T_{blv}) \tag{4}$$

where h_x is the counter-current heat exchange coefficient (W/K) for a specific segment. This study used h_x values from Fiala et al. [11]. The variable T_{blv} is the vein blood temperature; it can be determined by assuming equilibrium between the vein and the surrounding tissues:

$$T_{blv} = \sum_{layers} (\omega_{bl} VT) / \sum_{layers} (\omega_{bl} V) \tag{5}$$

Using Eqs. (3), (4), and (5), we can solve for ΔT_{bla} for extremity segments, and the T_{bla} can be determined sequentially for segments along the direction of arterial blood flow. The T_{blp} is calculated by the following equation, according to Fiala et al. [11]:

$$T_{blp} = \sum_{seg.} \left(\frac{(\rho_{bl} c_{bl} \sum_{layers} (\omega_{bl} V))^2}{\rho_{bl} c_{bl} \sum_{layers} (\omega_{bl} V) + h_x} T_{blv} \right) / \sum_{seg.} \left(\frac{(\rho_{bl} c_{bl} \sum_{layers} (\omega_{bl} V))^2}{\rho_{bl} c_{bl} \sum_{layers} (\omega_{bl} V) + h_x} \right) \tag{6}$$

2.5. Boundary conditions

To solve the bio-heat transfer equation (Eq. (1)), we need boundary conditions. The boundary of a human body is the skin surface. Thus, the heat flux between the skin surface and the surrounding environment (q_{sk}, W/m^2) should be specified. The q_{sk} consists of three parts, convection C (W/m^2), radiation R (W/m^2), and evaporation E_{sk} (W/m^2):

$$q_{sk} = C + R + E_{sk} \tag{7}$$

The convection and radiation are coupled with each other and can be expressed as [15]:

$$C + R = \frac{(T_{sk} - T_o)}{R_{cl} + 1/\, f_{cl}(h_c + h_r)} \tag{8}$$

where R_{cl} is the clothing thermal resistance (m^2K/W); f_{cl} the clothing area factor that accounts for the increased area due to clothing; T_{sk} the skin surface temperature (K); and T_o the operative temperature (K) that includes the effects of convection ($h_c T_a$), long-wave radiation ($h_r T_{sr}$), and short-wave radiation ($\alpha f_p s$) [11]. The T_o can be determined from:

$$T_o = \frac{h_c T_a + h_r T_{sr} - \alpha f_p s}{h_c + h_r} \tag{9}$$

where T_a is the ambient air temperature (K), T_{sr} the surface temperature of the surroundings (K), α the short-wave absorptivity of the body surface (skin or clothing surface), f_p the projected area factor that denotes the percentage of surface exposed to the short-wave radiation, s the short-wave radiation intensity (W/m^2), h_c the convective heat transfer coefficient ($W/m^2/K$), and h_r the radiative heat transfer coefficient ($W/m^2/K$).

Our model considered the variation in h_c in different segments by using the formulation from de Dear et al. [16], who performed detailed measurements of convection heat loss in different segments of a thermal manikin in a wind tunnel. They used the following equation to describe the relationship between h_c and air velocity v (m/s):

$$h_c = Bv^n \tag{10}$$

where B and n are segment-specific constants as defined in Table 1. These constants are different for standing and seated persons. The h_r is defined according to the Stefan-Bolzmann law:

$$h_r = \sigma \varepsilon_{sf} \varepsilon_{sr} \Psi_{sf-sr} (T_{sf}^2 + T_{sr}^2)(T_{sf} + T_{sr}) \tag{11}$$

where $\sigma = 5.67 \times 10^{-8}$ $W/m^2/K^4$ is the Stefan-Bolzmann constant; ε_{sf} and ε_{sr} the emissivity of a human surface and the surroundings, respectively; and $\Psi_{sf\text{-}sr}$ the view factor between the body surface and the surroundings. Because the "views" at some sectors of the human body are "blocked" by other segments, $\Psi_{sf\text{-}sr}$ is different for various parts of a body segment along the angular direction, and T_{sf} is the body surface temperature (K). The ε_{sf}, ε_{sr}, and $\Psi_{sf\text{-}sr}$ were obtained from Fiala [8]. If the body segment is not covered with clothing, T_{sf} is the skin temperature T_{sk}. Otherwise, T_{sf} is the clothing surface temperature T_{cl} calculated from T_{sk}:

$$T_{cl} = T_{sk} - (C + R)R_{cl} \tag{12}$$

Table 1
Constants for determining the convective heat transfer coefficient.

	Seated		**Standing**	
	B	**n**	**B**	**n**
Head	4.90	0.73	3.20	0.97
Face	4.90	0.73	3.20	0.97
Neck	4.90	0.73	3.20	0.97
Shoulders	11.40	0.64	10.05	0.63
Thorax	8.68	0.62	8.07	0.62
Abdomen	8.68	0.62	8.07	0.62
Upper arms	11.40	0.64	10.05	0.63
Lower arms	11.75	0.63	12.55	0.54
Hands	13.46	0.60	14.41	0.55
Upper legs	8.90	0.60	10.10	0.52
Lower legs	13.15	0.57	12.90	0.51
Feet	12.90	0.55	12.00	0.50

The evaporative heat loss at the skin, E_{sk}, depends on the difference in water vapor pressure at the skin and in the ambient environment [15]:

$$E_{sk} = w\frac{(P_{sk,s} - P_a)}{R_{e,cl} + 1/(f_{cl}h_e)} \tag{13}$$

where $P_{sk,s}$ is the saturated water vapor pressure (*kPa*) at the skin; P_a the water vapor pressure in the ambient air (*kPa*); and $R_{e,cl}$ the evaporative heat transfer resistance (m^2kPa/W), which is related to R_{cl} by the Lewis constant ($LR = 16.5\ K/kPa$) and clothing vapor permeation efficiency (i_{cl}) [15]:

$$R_{e,cl} = \frac{R_{cl}}{i_{cl}LR} \tag{14}$$

The h_e in Eq. (13) is the evaporative heat transfer coefficient ($W/m^2/kPa$) and is related to h_c by the Lewis constant:

$$LR = h_e / h_c \tag{15}$$

The w in Eq. (13) is the skin wetness, calculated by [15]:

$$w = 0.06 + 0.94E_{rsw} / E_{max} \tag{16}$$

where E_{rsw} is the heat loss through sweating (W/m^2), which is determined from the sweating thermoregulation mechanism [11]. The variable E_{max} is the maximum possible evaporative heat loss (W/m^2) and is calculated with the skin wetness set to 1.0 in Eq. (13).

Clothing serves as a barrier for heat and moisture transfer between the skin and the surrounding environment. Because the clothing coverage at one segment is different from that at another, the levels of clothing insulation at different local segments are not identical. Clothing insulation data, such as that in the ASHRAE handbook [15], can be applied only to the whole body. As a result, this study converted the whole body clothing resistance of a clothing element i ($R_{cl,whole,i}$, m^2K/W) to its local clothing resistance ($R_{cl,local,i}$, m^2K/W) by:

$$R_{cl,local,i} = \frac{A_t}{A_{cov,i}} R_{cl,whole,i} \quad (17)$$

where A_t is the total body surface area (m^2) and $A_{cov,i}$ the covered body area of clothing element i (m^2). The clothing thermal resistance at a local segment is the summation of $R_{cl,local,i}$ for all clothing elements on that segment. For unclothed segments, such as the head, face, neck, and hand, the value of R_{cl} is zero.

2.6. Numerical method

The finite-volume method with the fully implicit scheme [17] was used to discretize the bio-heat transfer equation. Convection and radiation were treated as mixed boundary condition [17] with the heat transfer coefficient as $1/(R_{cl}+1/f_{cl}(h_r+h_c))$ and the surrounding temperature as T_o. Evaporation was specified as Neumann boundary condition [17] by using E_{sk} as boundary heat flux. After the discrete equation set had been obtained, the tridiagonal matrix algorithm (TDMA) solver [17] was used to iteratively solve the temperature distribution within the human body.

3. Results

To evaluate the performance of the improved model proposed above, we compared the model's prediction of skin and core temperatures with experimental data from the literature. The evaluation was performed for scenarios that ranged from simple to complex. First, this study examined the model's performance under unclothed conditions so that the impact of clothing on the temperature could be eliminated. We then evaluated the model for cases with clothing but under uniform surrounding conditions. Finally, the model was examined for clothed subjects in non-uniform surroundings with asymmetric short-wave radiation.

3.1. Unclothed cases

Table 2 shows the conditions for five unclothed cases. The environment in these cases was the type that may be encountered in our daily life. The first case represented a situation in which people stayed in a typical indoor space with neutral thermal conditions. The second and third cases were transient with a moderate temperature change followed by a return to the initial conditions. These cases represented the dynamic processes that occur in springtime and autumn when people exit a neutral indoor space into a cool or warm outdoor space and then return to the indoor space. In the last two cases, the subjects experienced more dramatic changes from indoor to outdoor conditions. Typical winter and summer conditions were represented by air temperatures of 5^{o}C and 45^{o}C, respectively.

The evaluations compared the measured mean skin temperature $T_{sk,m}$ and rectal temperature T_{rec} with the calculated mean skin temperature and core temperature of the abdomen, which was used to approximate T_{rec}. The value of $T_{sk,m}$ was obtained by weighting the skin temperatures at different segments. The calculated $T_{sk,m}$ used weighting coefficients from Fiala et al. [11].

Table 2
Environmental conditions for the unclothed cases.

Case #	Environment	Air temp. (^{o}C)	Literature
1	Neutral	28	Stolwijk and Hardy [18]
2	Neutral-cool-neutral	28-18-28	Hardy and Stolwijk [19]
3	Neutral-warm-neutral	28-33-28	Stolwijk and Hardy [18]
4	Neutral-cold	28-5	Raven and Horvath [20]
5	Neutral-hot-neutral-hot	29-45-29-45	Yang et al. [21]

Figure 3 compares the measured and calculated $T_{sk,m}$ and T_{rec} for a case in which the subjects were in a neutral environment of 28^oC. It can be seen that even in a neutral environment, it was hard to achieve a steady state. During the four-hour experiment, the measured $T_{sk,m}$ decreased continuously for a total of about 1 K. The model was capable of calculating the decrease in $T_{sk,m}$, but only for 0.5 K. The calculated T_{rec} was about 0.25 K lower than the measured value. This is because the study used the core temperature of the abdomen to approximate the calculated T_{rec}. Since the rectum is located in the central region of the abdominal core, the rectal temperature should be higher than the core temperature.

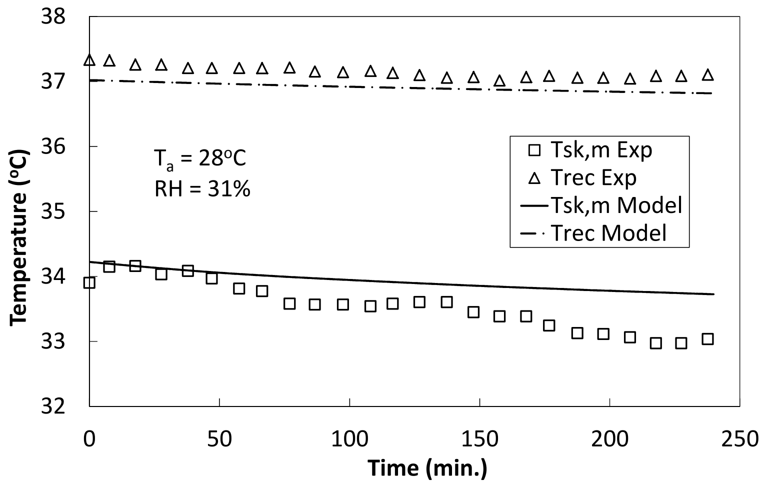

Fig. 3. Comparison of the calculated and measured mean skin temperature $T_{sk,m}$ and rectal temperature T_{rec} in an environment where the air temperature was at a neutral level [18].

Figure 4 compares the measured and calculated $T_{sk,m}$ and T_{rec} of the subjects when the surrounding conditions changed from neutral to cool and back to neutral (28-18-28^oC). At the beginning of the first neutral phase, there was a discrepancy between the measured and calculated $T_{sk,m}$. Because Hardy and Stolwijk [19] did not provide information about the environmental conditions before t = 0, this study assumed that the conditions were the same as in neutral phase 1. In the cooling phase and neutral phase 2, the change in the calculated $T_{sk,m}$ was not as rapid as that in the measured $T_{sk,m}$, which led to a 1.0 K difference. The difference may have been due to the use of circular cylinders to represent the body segments, which in reality are more like elliptical cylinders. A circular cylinder has a larger volume than an elliptical cylinder with the same surface area. For example, the total volume of the human body in this model was 71.8 liters, which is larger than the average volume of the male human body (63.0 liters) determined by Clauser et al. [22]. A larger volume would have led to greater "inertia" against the temperature change, and thus the change in the calculated $T_{sk,m}$ was not as rapid as that in the measured one. Similarly, the calculated T_{rec} values were lower than the measured data.

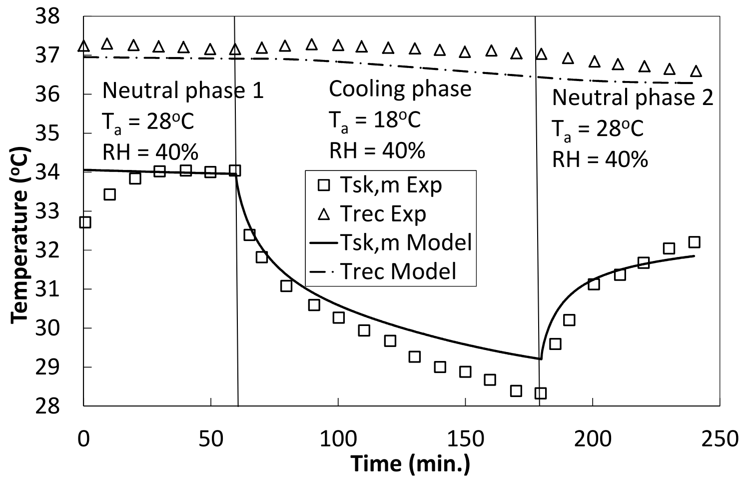

Fig. 4. Comparison of calculated and measured mean skin temperature $T_{sk,m}$ and rectal temperature T_{rec} in an environment where the air temperature changed from neutral to cool and back to a neutral level [19].

The measured $T_{sk,m}$ and T_{rec} of the subjects were also compared with the calculated values for an environment where the air temperature changed from neutral to warm and back to a neutral level, as shown in Figure 5. In neutral phase 1 and the heating phase, the calculated $T_{sk,m}$ values agreed well with the measured data. In neutral phase 2, the measured $T_{sk,m}$ decreased sharply, but the calculated $T_{sk,m}$ showed a flatter change, a trend which was similar to that in the case reported in the previous paragraph. The predicted T_{rec} was again slightly (0.3 K) lower than the measured one.

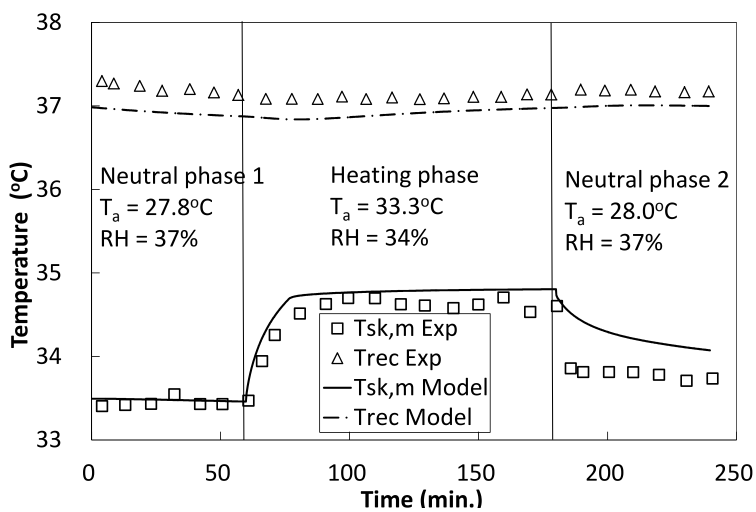

Fig. 5. Comparison of the calculated and measured mean skin temperature $T_{sk,m}$ and rectal temperature T_{rec} in an environment where the air temperature changed from neutral to warm and back to a neutral level [18].

The comparison shown in Figure 6 is for a case in which the subjects experienced a temperature change from neutral (28^oC) to cold (5^oC). In the neutral phase, the measured and calculated $T_{sk,m}$ and T_{rec} agreed well with each other. However, there was a notable difference between the measured and calculated T_{rec} in the cooling phase. The measured T_{rec} reached 37.9^oC, which seems abnormally high. This high T_{rec} may have been due to measurement uncertainties, as pointed out by Gordon et al. [23]. For $T_{sk,m}$ in the cooling phase, the calculated rates of change were always smaller than the measured rates, as explained in the discussion of the previous cases.

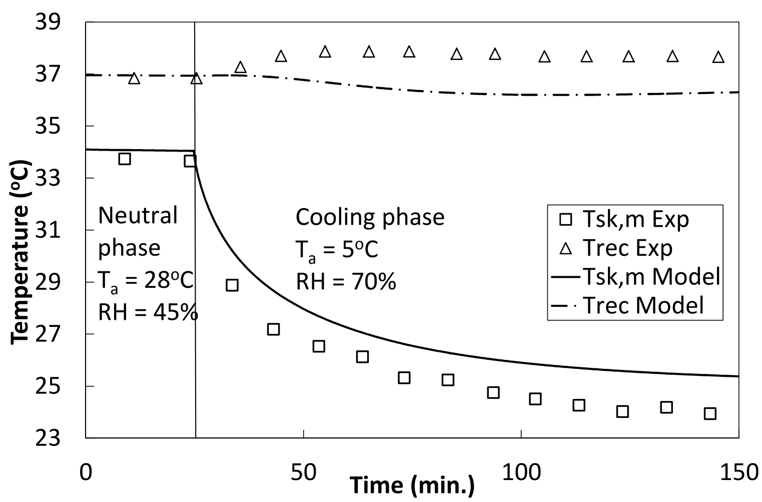

Fig. 6. Comparison of the calculated and measured mean skin temperature $T_{sk,m}$ and rectal temperature T_{rec} in an environment where the air temperature changed from neutral to a cold level [20].

Figure 7 compares the measured and calculated $T_{sk,m}$ and T_{rec} for subjects in an environment that alternated between neutral (29^oC) and hot (45^oC) conditions. In neutral phase 1, the calculated $T_{sk,m}$ values were about 0.4 K higher than the measured data. In the heating phases, the calculated change rate of T_{rec} was slightly lower than the measured rate. Yang et al. [21] quantified the intra-individual uncertainty in their measurements, as indicated by the error bars in Figure 7. This uncertainty was caused by the physiological variation among subjects. For example, a subject with a higher metabolic rate and more body fat would have a higher skin temperature. Our model addressed this variation by using averaged physiological data so that it yielded acceptable results, as one can see from Figure 7. The calculated $T_{sk,m}$ and T_{rec} were within the intra-individual uncertainty range.

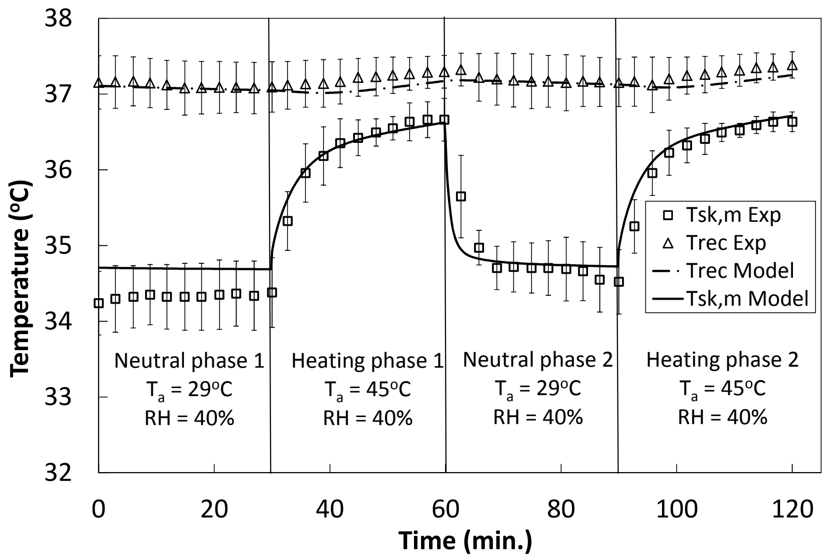

Fig. 7. Comparison of the calculated and measured mean skin temperature $T_{sk,m}$ and rectal temperature T_{rec} in an environment where the air temperature alternated between neutral and hot levels [21].

3.2. Clothed cases

After the model had been validated under unclothed conditions, we examined its performance when the subjects were clothed, which added some complexity to the modeling process. This investigation selected four experiments from the literature, as summarized in Table 3. In the first case, the subjects stayed in a neutral environment with a typical indoor air temperature. The environment in the second case was cold, simulating an outdoor space on a winter day. In the third case, the environment changed from neutral to hot. This situation may be experienced by people on a hot summer day when they walk outdoors from an indoor space. The environment in the last case alternated between extremely cold and extremely warm. This case was used to evaluate the model's dynamic response under dramatic environmental changes.

Table 3
Environmental conditions for the clothed cases.

Case #	Environ.	Air temp. (°C)	Clothes (clo)	Literature
1	Neutral	25.5	0.60	Olesen and Fanger [24]
2	Cold	10	1.90	Lee and Tokura [25]
3	Neutral-hot	28–40	0.31	Kakitsuba [26]
4	Cold-hot	-25–30	2.30	Ozaki et al. [27]

In the first case, 32 subjects stayed in a neutral environment of $25.5^{o}C$ for 2.5 hours. Figure 8 compares the measured and calculated skin temperature for different segments and the rectal temperature of the subjects. The skin temperature for the feet segment had the largest deviation, approximately 2 *K*. We found that in the calculation, the arterial temperature of the feet was about 3 *K* lower than the arterial temperature of the other segments. This was probably due to the high counter-current heat exchange coefficient h_x for the feet that was used in this study. The h_x was 3.4 *W/K* for the feet, while the value for the hands was only 0.57 *W/K*. Such a high h_x led to a large arterial temperature drop, which lowered the skin temperature of the feet. In the boundary condition calculation, we did not consider the heat conduction between the feet and the floor. This may be another reason for the underestimating the feet temperature. This measurement also contributed to the intra-individual uncertainty. The deviations between the predictions and measurements for all the segments were within the uncertainty range due to individual differences.

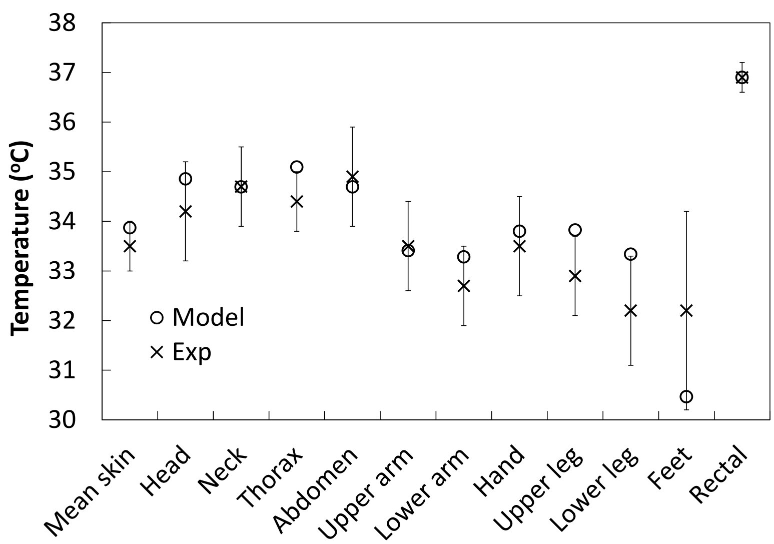

Fig. 8. Comparison of calculated and measured skin temperature for different segments and at the rectum in an environment where the air temperature was at a neutral level [24].

In the second case, the subjects stayed in a $10^{o}C$ environment for two hours. Figure 9 compares the calculated and measured skin temperatures for different segments of the subjects at the end of the 2-hour exposure period. Good agreement was found between the measured and calculated skin temperature, expect for the hand and foot segments. Once again, the skin temperature of the feet was underestimated by about 2 *K*. The skin temperature of the hands was overestimated by about 2.6 *K*. This overestimation may have been due to an overly high h_x for the feet and a too-low h_x for the hands.

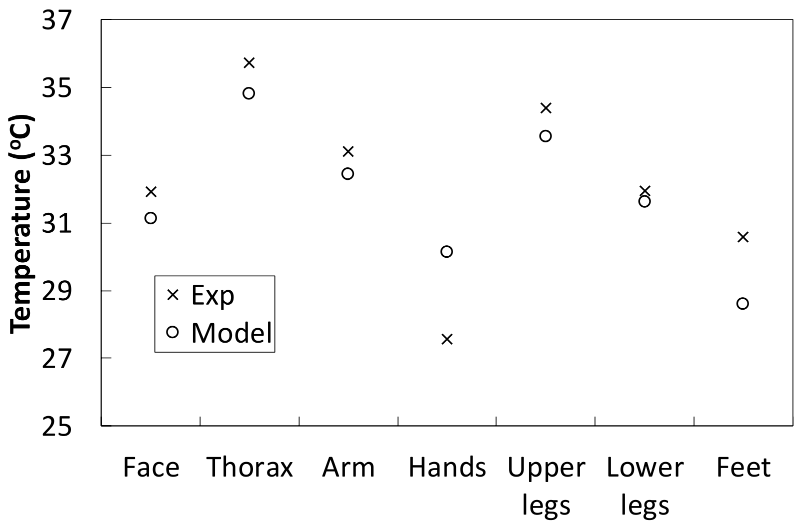

Fig. 9. Comparison of calculated and measured skin temperature for different segments in an environment where the air temperature was at a cold level [25].

The third case compared the measured and calculated $T_{sk,m}$ and T_{rec} of subjects who experienced an environmental change from neutral to hot, as shown in Figure 10. In the neutral phase, the calculated $T_{sk,m}$ was about 0.2 K higher than the measured $T_{sk,m}$. During the first 20 minutes of the heating phase, the measured $T_{sk,m}$ increased more rapidly than the calculated $T_{sk,m}$. However, during the remaining 40 minutes, the increase in the measured $T_{sk,m}$ slowed down and became slower than the increase in the calculated $T_{sk,m}$. The storage of sweat in the clothing may explain this difference. When the subjects entered the hot environment and began to sweat, their clothing absorbed the sweat, which reduced the heat loss through evaporation and accelerated the rate of increase in skin temperature. After about 20 minutes, the accumulated sweat penetrated the clothing, and evaporation increased at the clothing surface. The result was a slowdown in the skin temperature increase. Although our clothing model did not consider the absorption of sweat, the difference between the calculated and measured $T_{sk,m}$ was within 0.25 K. The calculated T_{rec} values were lower than the measured data, but the greatest difference was 0.3 K. These small differences may have been within the margin of error of the measurements.

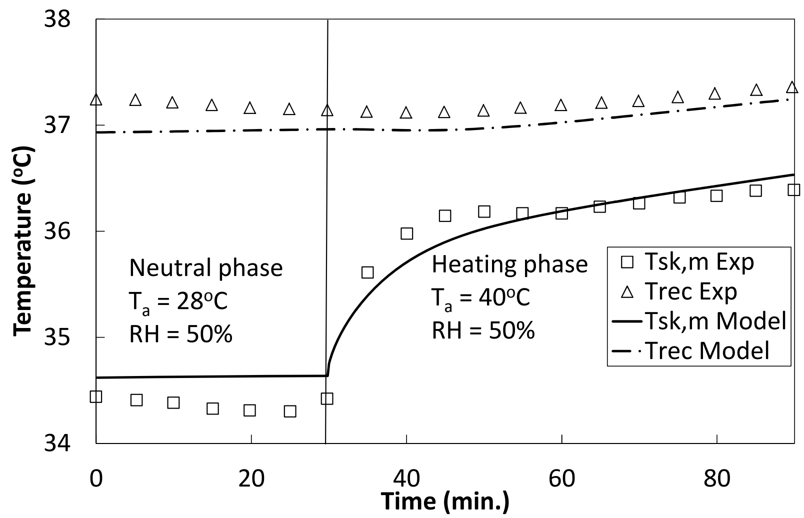

Fig. 10. Comparison of calculated and measured mean skin temperature $T_{sk,m}$ and rectal temperature T_{rec} in an environment where the air temperature changed from neutral to a hot level [26].

In the final case, after staying in a chamber with a temperature of 25^oC for 10 minutes, the subjects entered a chamber with an extremely cold air temperature, -25^oC, for 20 minutes. They were then transferred to a warm chamber with an air temperature of 30^oC for 20 minutes. Their stays in these cold and warm environments were repeated three times. Figure 11 compares the measured and calculated $T_{sk,m}$ of the subjects. The calculated $T_{sk,m}$ followed the measured data closely, but the calculated $T_{sk,m}$ changed more rapidly than the measured $T_{sk,m}$. This trend was different from that in the unclothed cases. The clothing insulation would have made a major contribution to the trend. For example, underestimation of the clothing insulation in the calculation would have caused the skin temperature to change more rapidly, as can be seen in Figure 11.

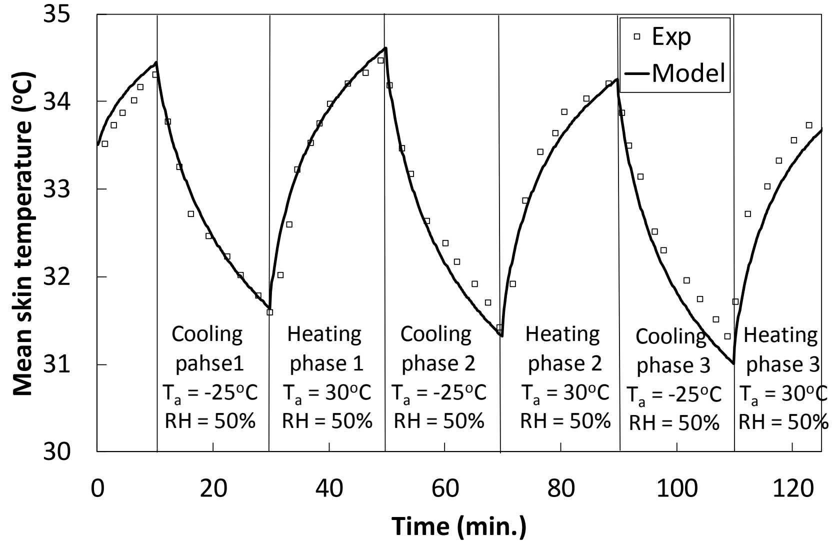

Fig. 11. Comparison of calculated and measured mean skin temperature $T_{sk,m}$ in an environment where the air temperature alternated between extremely cold and warm levels [27].

3.3. Cases with non-uniform short-wave radiation

In the previous cases, the surrounding environment was uniform. This section examines the model's performance for an environment with non-uniform short-wave radiation. This evaluation is important because, in outdoor spaces or vehicle cabins, people usually experience asymmetric short-wave radiation from the sun.

Hodder and Parsons [28] conducted an experiment to examine the effect of different intensities of solar radiation on skin temperature. They exposed the front part of the thorax, abdomen, arms, hands, and upper legs of eight clothed subjects to four levels of simulated solar radiation: 0, 200, 400, and 600 W/m^2. The asymmetric short-wave radiation would have caused a large skin temperature difference along the angular direction. However, the authors [28] did not state whether the skin temperature measurements were taken at locations facing the radiation source or shielded from the radiation. To account for this uncertainty, the present investigation calculated two values of $T_{sk,m}$ for the 200, 400, and 600 W/m^2 cases. One value was based on the skin temperature at locations facing the radiation, while the other was obtained from the skin temperature at locations shielded from the radiation.

Figure 12 compares the measured and calculated $T_{sk,m}$ of the subjects. Without short-wave radiation, the difference between the two was within 0.3 K. For the radiation levels of 200, 400, and 600 W/m^2, two lines are used in the figure to represent the two values of calculated $T_{sk,m}$: the upper line represents $T_{sk,m}$ calculated from the skin temperature at locations facing the radiation, while the lower line represents $T_{sk,m}$ at locations shielded from the radiation. The measured $T_{sk,m}$ agreed well with the upper calculated line, which suggests that the measurements were performed on sectors facing the radiation. The results also show that higher radiation intensity led to greater skin temperature asymmetry, as can be seen in a comparison of Figures 12(b), (c), and (d).

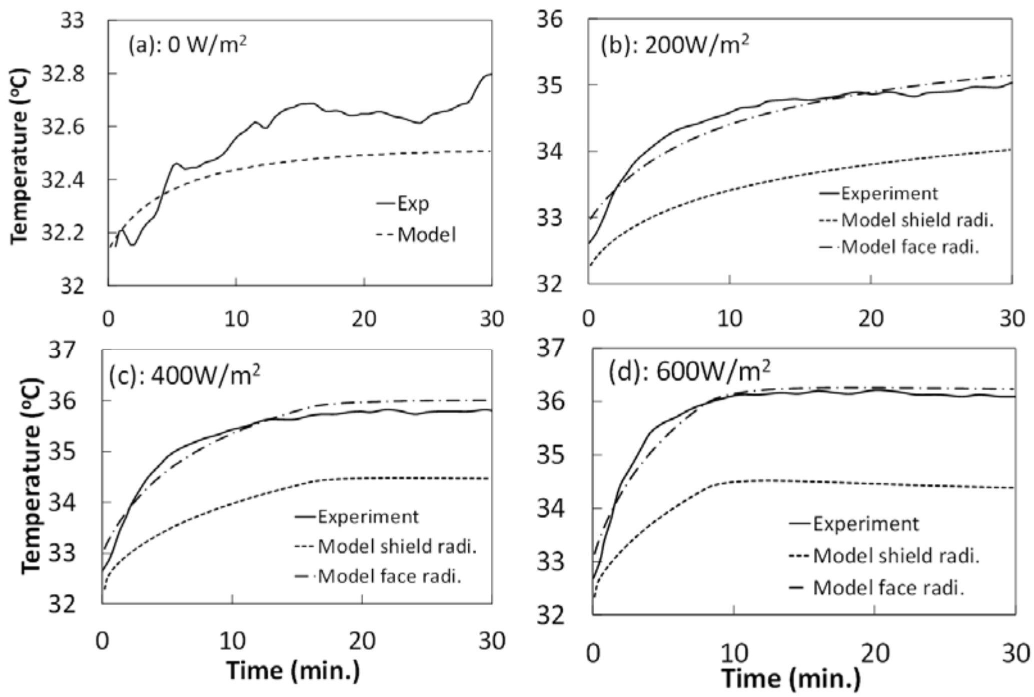

Fig. 12. Comparison of calculated and measured [28] mean skin temperature $T_{sk,m}$ in environments with different levels of short-wave radiation: (a) 0 W/m^2, (b) 200 W/m^2, (c) 400 W/m^2, and (d) 600 W/m^2.

4. Discussion

The measurements presented in this paper were all conducted in indoor spaces. It is unclear whether or not the same results would be obtained if a similar experiment were performed outdoors, the thermal environment would be more complex than that in an indoor space. Direct solar radiation imposes non-uniform heat transfer on the human body, while transient wind conditions lead to unsteady convection. Another complexity arises from the sudden change in environmental conditions when the human body enters an outdoor space from an indoor space or vice versa.

The effects of these complexities on human body temperature have not been experimentally investigated in previous studies. Although some studies have used models to numerically study the dynamic changes in skin and body core temperature [29, 30] in outdoor spaces, these investigations have not been validated because of a lack of corresponding experimental data. Therefore, in order to provide data to validate the human thermal models, it is proposed that measurements of human body temperature be conducted in outdoor spaces.

5. Conclusion

This investigation developed a multi-segment model for calculating thermal conditions in the human body on the basis of Fiala's work. The model uses two-dimensional heat transfer in the radial and angular directions. It takes into account the arterial blood temperature drop along the extremities due to counter-current heat exchange and the estimated clothing insulation at local segments based on the clothing insulation data for the whole body.

This study evaluated the model's performance for unclothed and clothed subjects under a wide range of environmental conditions, including non-uniform short-wave radiation. Generally, good agreement was observed between the calculated and measured skin and rectal temperatures. However, the calculated mean skin temperatures had a low change rate compared with the measured temperatures when the subject experienced a change in the surrounding environmental conditions. This difference may have been caused by the overestimation of body volume, since the model used circular cylinders to represent the body segments. The calculated hand and foot temperatures differed from the measured temperatures to a greater extent than those for the other body segments, possibly because the counter-current heat exchange coefficient had not been accurately determined in the model.

Acknowledgement

This research was partially supported by a special fund of the Key Laboratory of Eco Planning & Green Building, Ministry of Education (Tsinghua University), China, and the China Scholarship Council (CSC).

References

[1] P.O. Fanger, Thermal comfort. Analysis and Applications in Environmental Engineering, McGraw-Hill, New York, 1970.

[2] A.P. Gagge, An effective temperature scale based on a simple model of human physiological regulatory response, ASHRAE Trans. 77 (1971) 247-262.

[3] P. Höppe, The physiological equivalent temperature–A universal index for the biometeorological assessment of the thermal environment, Int. J. Biometeorol. 43 (1999) 71-75.

[4] D. Lai, D. Guo, Y. Hou, C. Lin, Q. Chen, Studies of outdoor thermal comfort in northern China, Build. Environ. 77 (2014) 110-118.

[5] J.A.J Stolwijk, A mathematical model of physiological temperature regulation in man, NASA contractor report, NASA CR-1855, Washington DC, 1971.

[6] Y. Cheng, J. Niu, N. Gao, Thermal comfort models: A review and numerical investigation, Build. Environ. 47 (2012) 13-22.

[7] C. Huizenga, H. Zhang, E. Arens, A model of human physiology and comfort for assessing complex thermal environments, Build. Environ. 36 (2001) 691-699.

[8] D. Fiala, Dynamic simulation of human heat transfer and thermal comfort, PhD thesis, De Montfort University, UK, 1998.

[9] D. Fiala, K.J. Lomas, M. Stohrer, A computer model of human thermoregulation for a wide range of environmental conditions: The passive system, J. Appl. Physiol. 87 (1999) 1957-1972.

[10] D. Fiala, K.J. Lomas, M. Stohrer, Computer prediction of human thermoregulatory and temperature responses to a wide range of environmental conditions, Int. J. Biometeorol. 45 (2001) 143-159.

[11] D. Fiala, G. Havenith, P. Bröde, B. Kampmann, G. Jendritzky, UTCI-Fiala multi-node model of human heat transfer and temperature regulation, Int. J. Biometeorol. 56 (2012) 429-441.

[12] H.H. Pennes, Analysis of tissue and arterial blood temperatures in the resting human forearm, J. Appl. Physiol. 1 (1948) 93-122.

[13] P.O. Fanger, Calculation of thermal comfort: Introduction of a basic comfort equation, ASHRAE Trans. 73 (1967) 1-20.

[14] R.G. Gordon, The response of human thermoregulatory system in the cold, PhD thesis, University of California, Santa Barbara, USA, 1974.

[15] ASHRAE, ASHRAE Handbook, Fundamentals, American Society of Heating, Refrigerating and Air-conditioning Engineers, Inc., Atlanta, 2009.

[16] R.J. de Dear, E. Arens, H. Zhang, M. Oguro, Convective and radiative heat transfer coefficients for individual human body segments, Int. J. Biometeorol. 40

(1997) 141-156.

[17] S. Patankar, Numerical Heat Transfer and Fluid Flow, CRC Press, Boca Raton, 1980.

[18] J.A.J Stolwijk, J.D. Hardy, Partitional calorimetric studies of responses of man to thermal transients, J. Appl. Physiol. 21 (1966) 967-977.

[19] J.D. Hardy, J.A.J. Stolwijk, Partitional calorimetric studies of man during exposures to thermal transients, J. Appl. Physiol. 21 (1966) 1799-1806.

[20] P.R. Raven, S.M. Horvath, Variability of physiological parameters of unacclimatized males during a two-hour cold stress of 5ºC, Int. J. Biometeorol. 14 (1970) 309-320.

[21] J. Yang, W. Weng, B. Zhang, Experimental and numerical study of physiological responses in hot environments, J. Therm. Biol. 45 (2014) 54-61.

[22] C.E. Clauser, J.T. McConville, Young JW, Weight, volume, and center of mass of segments of the human body, Wright-Patterson Air Force Base, Yellow Springs, Ohio, 1969.

[23] R.G. Gordon, R.B. Roemer, S.M. Horvath, A mathematical model of the human temperature regulatory system-transient cold exposure response, IEEE Trans. Biomed Eng 23 (1976) 434-444.

[24] B.W. Olesen, P.O. Fanger, The skin temperature distribution for resting man in comfort, Arch. Sci. Physiol. 27 (1972) 385-393.

[25] H.Y. Lee, H. Tokura, Thermophysiological significance and the role of local clothing in ambient 10ºC environments, Appl. Human Sci. 17 (1998) 19-26.

[26] N. Kakitsuba, Dynamic changes in sweat rates and evaporation rates through clothing during hot exposure, J. Therm. Biol. 29 (2004) 739-742.

[27] H. Ozaki, H. Enomoto-Koshimizu, Y. Tochihara, K. Nakamura, Thermal responses from repeated exposures to severe cold with intermittent warmer temperatures, Appl. Human Sci. 17 (1998) 195-205.

[28] S.G. Hodder, K. Parsons, The effects of solar radiation on thermal comfort, Int. J. Biometeorol. 51 (2007) 233-250.

[29] P. Höppe, Different aspects of assessing indoor and outdoor thermal comfort, Energy Build. 34 (2002) 661-665.

[30] G. Katavoutas, H.A. Flocas, A. Matzarakis, Dynamic modeling of human thermal comfort after the transition from an indoor to an outdoor hot environment, Int. J. Biometeorol. 59 (2015) 205-216.